Chemistry–A European Journal
Review
doi.org/10.1002/chem.202202722
Chemistry Europe
European Chemical Societies Publishing
www.chemeurj.org

Stability of Catalytic Centres in Light-Driven Hydrogen Evolution by Di- and Oligonuclear Photocatalysts

Martin Lämmle,[a] Alexander K. Mengele,[a] Georgina E. Shillito,[b] Stephan Kupfer,[b] and Sven Rau*[a]

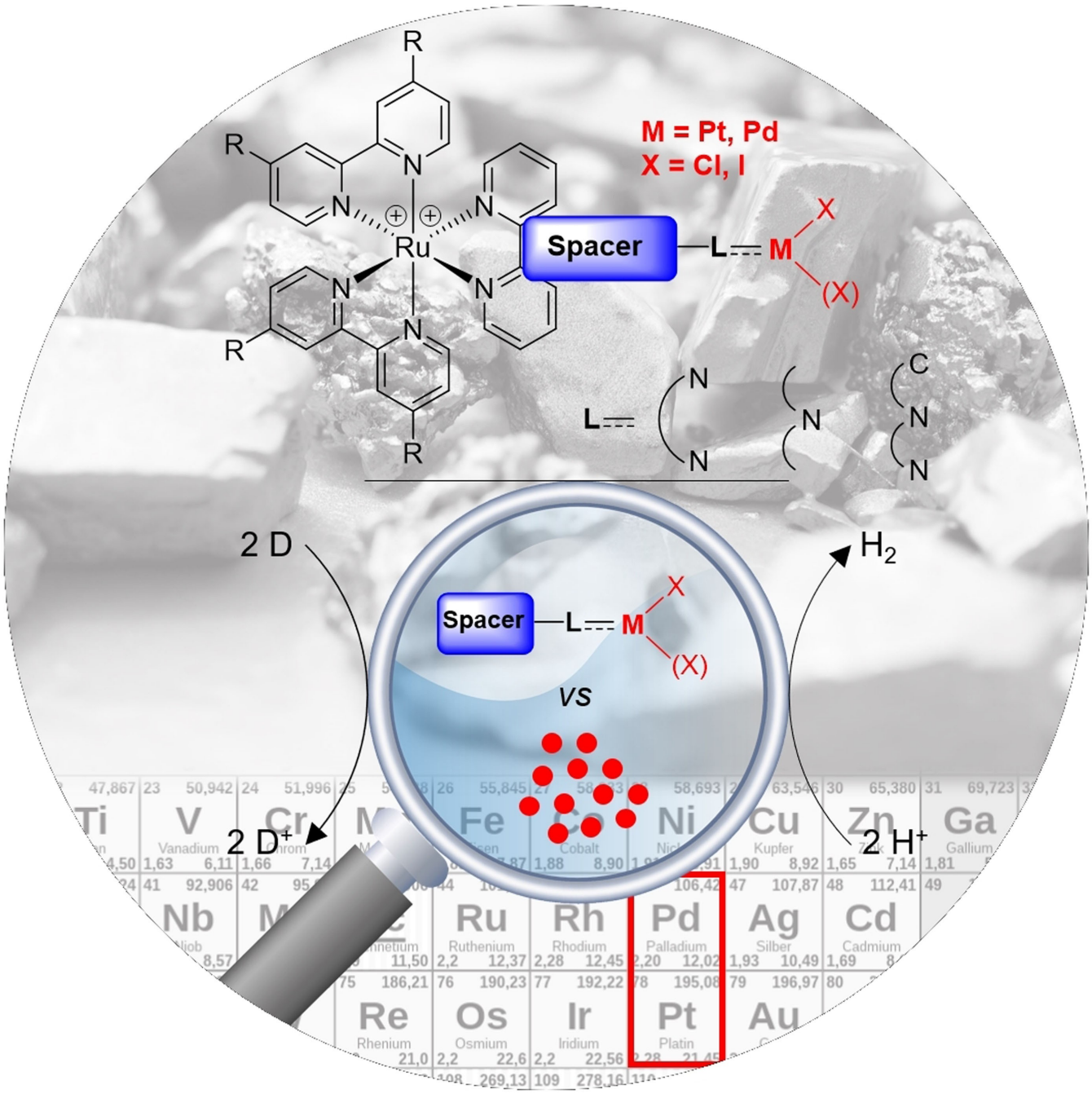

Abstract: A review. In recent decades, mimicking natural photosynthesis by artificial photocatalysis represented a major research direction with the ultimate goal of reducing fossil fuel consumption through efficient solar energy harvesting. To transfer molecular photocatalysis from the lab scale to an industrially relevant process, it is important to overcome instability problems of the catalysts during light-driven operation. As it is well-known that many of the typically utilized noble metal-based catalytic centres (e.g. Pt and Pd) undergo particle formation during (photo)catalysis and thus switch the whole process from a homogeneous into a heterogeneous one, an understanding of the factors governing particle formation is crucially needed. The review therefore focuses on di- and oligonuclear photocatalysts bearing a range of different bridging ligand architectures for drawing structure-catalyst-stability relationships in light-driven intramolecular reductive catalysis. In addition, ligand effects at the catalytic centre and their implications for catalytic activity in intermolecular systems will be discussed, as will important insights into the future design of operationally stable catalysts.

1. Introduction

The switch from fossil fuels to renewable energies is the key aspect to limit global warming to 1.5 °C compared to preindustrial times, as carbon dioxide is one of the main greenhouse gases, next to CO and methane.[1,2] However, the actual CO_2 concentration in the atmosphere is the highest within the past 800,000 years, going in hand with the rise of the sea levels as well as the temperature.[3,4] Since the early 19th century, the amount of fossil fuels used for energy production continuously increased.[5–7] Already in 1912, G. Ciamician realized that coal is nothing other than solar energy in its concentrated form. With this statement and his groundbreaking work, G. Ciamician can be considered as a pioneer of modern photochemistry.[8]

Compared to other renewable energy sources (e.g. wind, geothermal, …), solar radiation provides a tremendous amount of energy as around 4×10^{24} J reaches the earth per year, from which 5×10^{22} J could be easily harvested.[9] However, the main disadvantage of renewable energies – no continuous availability – hinders the efficient utilization to some point. To completely replace fossil fuels with renewable energies, it is important to provide sufficient storage possibilities.[10–12]

The key to increasing the availability of renewable energies is the efficient capture and conversion of solar energy into chemical energy by mimicking natural photosynthesis. In artificial photosynthesis organic components undergo reduction (e.g. H_2O to H_2; CO_2 to CO, CH_4; …), comparable to the reduction of CO_2 to carbohydrates in natural photosynthesis, while oxidation of water to O_2 still remains as the economically best suited oxidative half reaction.[13,14]

Thus, photolytic splitting of water into H_2 and O_2 (see Scheme 1) is valued, as H_2 is one very promising energy storage candidate as it provides a high energy density (119.8 MJ kg^{-1}),[15] it burns with high temperature,[16] can be used in fuel cells for traffic and heating as well,[17,18] provides sufficient storability in large amounts[16] and can be produced from water.[19,20] However, in 2015, up to 96% of the produced hydrogen was still generated out of fossil fuels (so called grey hydrogen) and only a small amount (up to 4%) was directly produced from water via renewable energy-driven electrolysis (green hydrogen).[21,22] This can mainly be attributed to higher prime costs for the production of green hydrogen (2016: wind power-driven electrolysis 6.64 $US/kg) compared to fossil fuels (2016: 0.93–1.22 $US(kg).[22]

A possible solution to overcome the economic bottleneck in renewable energy-driven hydrogen evolution are hetero- or homogeneous photocatalysts based on earth abundant materials which harvest light energy efficiently and produce hydrogen as solar fuel. Up to now, homogeneous systems often under-

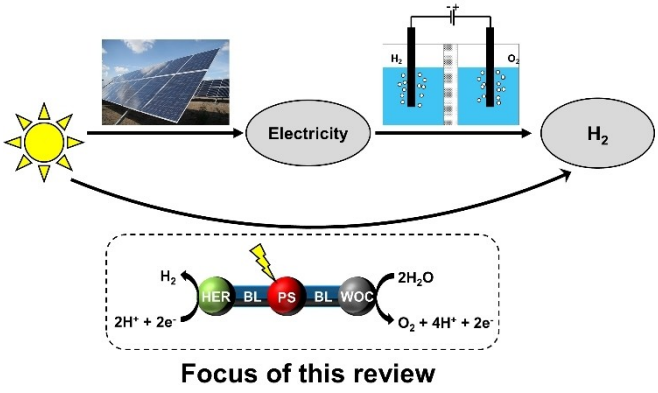

Scheme 1. Green hydrogen formation by electrolysis (top) and by direct utilization of light for water splitting by artificial photosynthesis (bottom).[23–26] HER = hydrogen evolution reaction centre, BL = bridging ligand, PS = photosensitizer, WOC = water oxidation centre.

[a] *M. Lämmle, Dr. A. K. Mengele, Prof. Dr. S. Rau*
Institute of Inorganic Chemistry I
Ulm University
Albert-Einstein-Allee 11, 89081 Ulm (Germany)
E-mail: sven.rau@uni-ulm.de

[b] *Dr. G. E. Shillito, Dr. S. Kupfer*
Institute of Physical Chemistry
Friedrich Schiller University Jena
Helmholtzweg 4, 07743 Jena (Germany)

Selected by the Editorial Office for our Showcase of outstanding Review-type articles (www.chemeurj.org/showcase).

went side reactions during catalysis and proved to be rather inefficient in hydrogen evolution compared to heterogeneous systems. However, the utilization of homogeneous systems allows for the detailed investigation of the catalytic mechanism and opens up the possibility for the development of a rational design strategy. A very useful approach along these lines is the ligand-based finetuning of electron transfer and hydrogen evolution efficiency, respectively. However, to achieve this, the photo-responsive and catalytically active molecular components employed, need to exhibit excellent stability under operating conditions. In oligonuclear photocatalytic systems, the processes of light absorption and catalytic turnover can be combined in individual molecules (intermolecular) or within one molecular architecture (intramolecular, see some examples in Figure 1).[27–32] As the intramolecular systems pose some beneficial aspects such as efficient forward electron transfer, this review will focus on different di- and oligonuclear systems exhibiting different bridging ligand (BL) architectures and details regarding structural parameters that beneficially impact the stability of these systems.[33,34]

2. Artificial Photosynthesis

One of the main components of artificial photosynthetic systems is a photosensitizer (PS) – comparable to the chlorophyll and carotenoid parts in natural photosynthesis – which harvests light energy by absorption of a photon in the ground state (GS) which induces the population of a redox-active electronically excited state from which charge separation occurs.

Charge separation is typically mediated by means of an electron relay R (intermolecular system, for example methylviologen,[39–41]) or a BL (intramolecular system). In the case of

Martin Lämmle studied chemistry at Ulm University from 2014 on. After receiving his master's degree in 2019, he started his PhD under the supervision of Prof. Dr. Sven Rau. His research focuses on the synthesis and characterization of novel dinuclear photocatalysts, suitable for photocatalytic water reduction. Further, he investigates the effect of varying bridging ligand architectures on the photocatalytic and photophysical properties of ruthenium metal complexes.

Alexander Mengele studied chemistry and business chemistry at Ulm University, Germany, from 2010–2015. After receiving his PhD in 2021 under the guidance of Prof. Dr. Sven Rau, Alexander Mengele continued to work as scientific employee in his group and focuses on photocatalytic applications of oligonuclear coordination compounds for water splitting and photoactive compounds for photobiocatalytic applications such as light-driven NADH as well as ATP formation. He is also utilizing supramolecular chemistry to accelerate selective NADH photooxidations for NAD^+-driven enzymatic oxidations.

Georgina E. Shillito completed her PhD at the University of Otago in 2019 under the supervision of Professor Keith Gordon, specialising in the spectroscopy of photoactive molecules. She then worked as a postdoc in Raman spectroscopy and optics at the University of St Andrews in the UK and is currently a member of the Quantum Chemistry sub-group of Dr Stephan Kupfer at Friedrich Schiller University Jena.

Stephan Kupfer received his PhD in 2013 from the Friedrich-Schiller-University Jena, Germany, where he is currently a group leader in the Physical Chemistry Department. His research is focused on the theoretical modelling of photo-induced processes, i.e., in the fields of solar energy conversion and energy storage systems. For light-harvesting applications, either in the scope of (dye-sensitized) solar cells or light-driven water-splitting, detailed understanding of the fundamental photophysics and photochemistry is of uttermost importance. Therefore, he aims to elucidate as well as to tune excited state relaxation dynamics in (supra)molecular photocatalysts and light-harvesting antenna associated to electron and energy transfer processes, i.e., charge separation, charge recombination and photodegradation.

Sven Rau studied chemistry at the Friedrich-Schiller-University of Jena and Dublin City University. He obtained his Diploma in chemistry in 1997 and his PhD in 2000. Following his habilitation in 2007, he took on a W 2 professorship at the Friedrich-Alexander-University Erlangen-Nuremberg in 2008. Since 2011, he leads the institute for materials and catalysis at Ulm University. Since 2018 he has been spokesperson of the CRC CataLight and since 2022 he is co-spokesperson. His research interests are on the synthesis and characterization of photoredoxactive metal complexes, their applications in light-driven catalytic conversions, photoelectrochemistry, and photodynamic therapy.

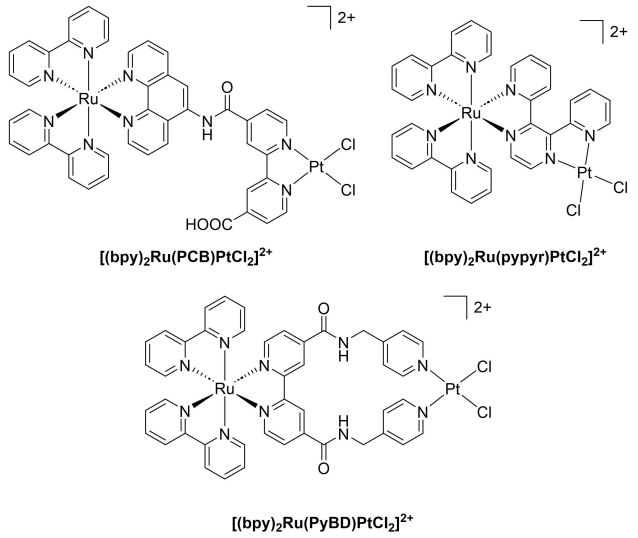

Figure 1. Examples for intramolecular artificial photosynthetic systems investigated by Sakai et al.[35–38] PCB = 4′-((1,10-phenanthrolin-5-yl)carbamoyl)-[2,2′-bipyridine]-4-carboxylic acid, pypyr = 2,3-di(pyridin-2-yl)pyrazine, PyBD=N4,N4′-bis(pyridin-4-ylmethyl)-[2,2′-bipyridine]-4,4′-dicarboxamide.

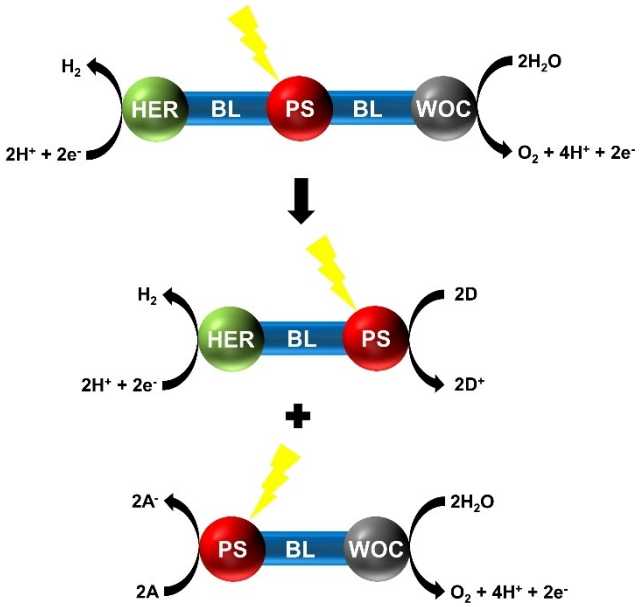

Figure 2. Schematic separation of the HER-BL-PS-BL-WOC triade (top) into two separated half reactions for proton reduction (HER, left) and water oxidation (WOC, right). To substitute the missing half reaction electron donors (for HER, i.e. TEOA, TEA) or electron acceptors (for WOC, i.e. $Na_2S_2O_8$) have to be used.

intermolecular systems, the electron is transferred from an electronically excited state of the PS onto the electron relay (R) via a hopping mechanism, while the intramolecular approach benefits from the possibility of direct light-driven charge transfer from the PS to the BL. Additionally, spectroscopic and theoretical tools can be employed to study such well-defined systems, yielding a greater depth of understanding. Eventually, the electron is further transferred to the hydrogen evolution reaction (HER) centre, where molecular hydrogen is produced. The now oxidized PS can be reduced by electrons transferred via electron relays or BLs, from the active centre for water oxidation catalysis (WOC), which oxidizes water to form molecular oxygen and protons as well (see Figure 2 (top)).[13,42,43] It is important that the lifetime of the excited state is sufficiently long to allow charge separation via efficient intramolecular electron transfer. However, due to the molecular connection of the PS and the catalyst it is possible to function with significantly lower excited state lifetimes in PS-BL-CC-based systems (CC = catalytic centre) compared to the lifetimes needed for intermolecular catalysis, which is especially important for earth abundant 3d metals as PS (e.g. Fe).[44–48]

However, an efficient combination of a 4-electron oxidation with a 2-electron reduction is difficult to achieve, as under these conditions, the released hydrogen can be re-oxidized by the WOC and the oxygen reduced by the HER or other highly reducing intermediates of the system. Detrimental effects of oxygen on the HER activity have been discussed extensively.[49,50]

Therefore splitting the overall catalysis into oxidation and reduction parts enables and simplifies the exclusive optimization of every single half-reaction (see Figure 2 (bottom)).[51] Consequently, the systematic variation of the PS, CC as well as the substitution pattern, the energetic levels and steric parameters of the BL architecture yields important insights into how these systems have to be further optimized. As a result of splitting the overall reaction into separate processes, the respective other half-reaction has to be replaced by utilization of sacrificial electron acceptors (e.g. $Na_2S_2O_8$, $[Co(NH_3)_5Cl]Cl_2$, …)[52–55] or electron donors (e.g. triethylamine, triethanolamine, …),[56,57] respectively.

In intramolecular water reduction catalysis, the PS is typically represented by a transition metal-based chromophoric unit while the CC consists of noble metals (e.g. Pt, Pd). The PS in reductive catalysis is often coordinated by an N,N-coordination sphere while for the catalytic active centre N,N-chelating and N-heterocyclic carbene (NHC) ligands are predominant in literature.[58–61]

As already mentioned above, the BL architecture is crucial for efficient catalysis. In detail, the BL has to consist of two coordination spheres that are able to stabilize the PS and CC, respectively (see Figures 2 and 3). The BL has to stabilize the CC under reductive conditions with varying oxidative states (starting oxidation state and lower oxidation states due to charge accumulation prior to hydrogen evolution) to prohibit reduction-induced colloid formation and the associated switch from truly molecular to heterogeneous photocatalysis. In oligonuclear systems, both coordination spheres, i.e. the ligand sphere at the PS and the ligand moiety at the CC, have to be connected to each other via different linkers. Interruption of the conjugation by introduction of an alkyl moiety or a triazole unit can be achieved, while planar connection can result in conjugated systems (see Figure 3). However, not only C–C bonds but also amide-linkages formed by the reaction of an

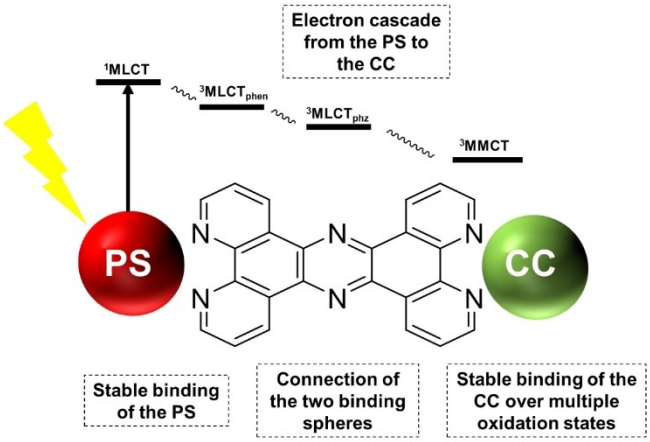

Figure 3. Important properties of the BL architecture in case of the tpphz-BL (tpphz = tetrapyrido[3,2-*a*:2′,3′-*c*:3″,2″-*h*:2‴,3‴-*j*]phenazine).[60]

amine with a carboxylic acid can be used for the molecular connection of PS and CC subunits.[62]

Besides influencing the photophysical properties of these systems,[63,64] these different connection techniques also significantly influence the stability of the BL against pH, temperature and irradiation as well as the stability of the CC during light-driven catalysis.

Furthermore, substitution of the respective coordination spheres with bulky or electron donating/withdrawing groups (e.g. *tert*-butyl, …) can directly influence the photocatalytic activity.[65] These groups can either influence the electronic situation at the PS,[66] the steric demand at the CC and/or raise or lower the energies of the respective orbitals of the BL, allowing a higher driving force for the electron transportation and the stable binding of the CC.

3. Mechanism of Electron Transfer and HER

As already mentioned above, it is important that efficient electron transfer from the PS to the CC occurs to provide efficient catalysis. Therefore, mechanistic insight with respect to the electron transfer as well as the subsequent hydrogen formation is of great interest. A very thorough theoretical description of a photocatalytic system including a square planar (NN)$PdCl_2$ catalytic unit (NN = α-diimine ligand), strongly related to the (NN)$PtCl_2$ already shown in Figure 1 utilizes the [(tbbpy)$_2$Ru(tpphz)$PdCl_2$] (tpphz = tetrapyrido[3,2-*a*:2′,3′-*c*:3″,2″-*h*:2‴,3‴-*j*]phenazine) intramolecular photocatalyst.[67] This catalytic system shows light-induced hydrogen formation and will be discussed in detail at a later stage. Theoretical studies on [(tbbpy)$_2$Ru(tpphz)$PdCl_2$] revealed that after photon absorption, metal-to-ligand charge transfer ($MLCT_{BL}$) states were accessible, allowing for a direct photo-reduction of the BL.[68] However, no electron- but rather energy transfer from the $^3MLCT_{BL}$ state to a metal-centred ($^3MC_{Pd}$) state was observed. Depending on the energy of the antibonding $\sigma^*_{x^2-y^2}$-orbital, which is populated in these $^3MC_{Pd}$ states and mainly involves the $d_{x^2-y^2}$ orbital of the CC and the lone-pairs of the coordinating ligands, weakening of the metal-halide bond occurs.

After ligand loss and (potential re−)excitation of the Ru centre, electron transfer via metal-to-metal charge transfer states (^{3}MMCT) becomes energetically favourable, which leads eventually to the photo-reduction of the CC (see Scheme 2),[68] i.e., yielding the reduced Pd(I)Cl intermediate. These more detailed theoretical investigations also support the initial experimental finding which indicated a localisation of the electron after photochemical reduction on the palladium centre which had lost a chloride ligand. The more recently developed quantum chemically derived mechanism allows to rationalize experimental data, as addition of halide salts (e.g. tetrabutylammonium chloride) to [(tbbpy)$_2$Ru(tpphz)$PdCl_2$]$(PF_6)_2$ under catalytic conditions causes deactivation of hydrogen evolution.[60]

It might also be assumed, that [(tbbpy)$_2$Ru(tpphz)$PtCl_2$]$(PF_6)_2$ would react similarly, i.e., activation of the CC by energy transfer followed by a subsequent electron transfer event. However, in this case, the $^3MLCT_{BL}$ to ^{3}MMCT population transfer rate constant would only be about $10^{-7}\,s^{-1}$ (very low compared to the $PdCl_2$ analogue with $k \approx 10^7\,s^{-1}$) mainly caused by the higher energy of the ^{3}MMCT states by ca. 0.8–0.9 eV. In contrast to [(tbbpy)$_2$Ru(tpphz)$PdCl_2$], also the $^3MC_{Pt}$ states that may lead to a stabilization of the electron accepting $\sigma^*_{x^2-y^2}$-orbital of the CC upon weakening of the metal-halide bond are also much higher in energy and are therefore only slowly populated in [(tbbpy)$_2$Ru(tpphz)$PtCl_2$] as well.[69] Thus, instead of chloride dissociation, backwards electron transfer from $^3MLCT_{BL}$ follows, causing low catalytic activity and no influence of excess chloride under catalytic conditions.[60] Further, the BL architecture has, to a certain degree, influence on the chemical stability of the photoactive PS unit. By this, small changes of the catalyst might have a tremendous effect on the actual hydrogen evolution mechanism. As the tpphz ligand is redox active itself, it should be noted that it is so far not completely understood how the mechanism of CC reduction changes in case of a

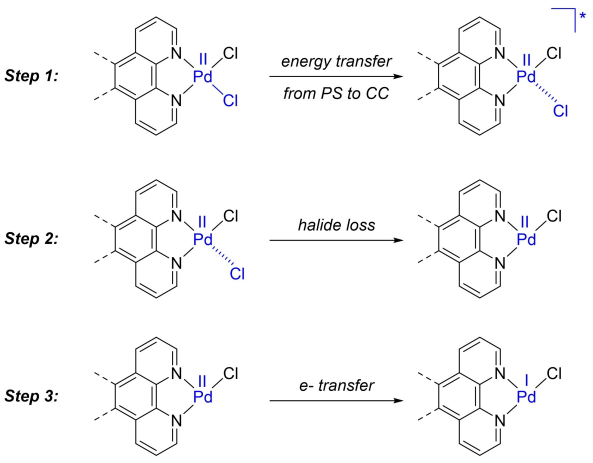

Scheme 2. Schematic mechanism of the electron transfer and photocatalytic HER of the catalytically active site of [(tbbpy)$_2$Ru(tpphz)$PdCl_2$]$(PF_6)_2$ based on theoretical investigations.[68]

mono-reduced BL which has been proposed to form within minutes under catalytic conditions.[49] As a result, additional research must be conducted in the near future to provide a clearer picture on the mechanism of electron transfer as well as on the actual hydrogen evolution at the reduced and active CC.

4. Instability of the Catalytic Metal Centre as a Limiting Factor in Artificial Photosynthesis

In di- or oligonuclear catalytic systems, consisting at least of one PS and one CC, catalytic turnover can proceed by either a fully molecular or colloid-driven (heterogeneous) mechanism. The latter represents the loss of the CC from the molecular PS-BL-CC precatalyst after reduction of the CC. In this case the synthesized oligonuclear system serves as precursor for the catalytic system.

As already indicated above, one of the main decomposition routes for noble metal-containing photocatalysts (Pt or Pd as CC) during photocatalysis is the loss of the CC and subsequent particle formation.[35,60,70] These mostly colloidal metal-nanoparticles are able to act as catalysts as well. This renders the overall light-induced hydrogen evolving catalytic system particle size-dependent, provided the remaining PS-BL system retains its function.[71,72] The standard procedure to evaluate whether particle formation occurs or not is to perform catalysis in the presence of elemental mercury which nearly quantitatively reacts with the in situ formed metal particles by formation of an amalgam.[62,73] These particles are then inhibited for further hydrogen evolution during irradiation.[74]

In the presence of elemental Hg, a colloid-driven catalysis typically provides significantly reduced catalytic activity (ideally zero activity).[75,76] As Chernyshev et al. and other groups could show, it is mandatory to perform the Hg test under controlled conditions (e.g. stirring speed, Hg loading, …) as otherwise, false conclusions may be drawn.[75–78] Thus, Hg-accelerated reduction of the CC and subsequent Hg-induced decomplexation has to be ruled out by testing the stability of the pure compound on Hg. By stirring the compound in the presence of Hg in the pure solvent, excluding irradiation, and measuring NMR before and after a given time interval, the stability of the compound against pure Hg can be evaluated. It should be noted that it is very important to exclude direct deactivation of the catalyst by Hg(0).[75,79,80] The following effects of elemental Hg on a PS-BL-CC system, such as i) loss of ligand environment at the CC[81] and ii) loss of the whole CC[60] have already been observed. Furthermore, Hg(0) may for instance reduce the photo-oxidized $[Ru(III)(bpy)_3]^{3+}$ (bpy = 2,2′-bipyridine) complex under formation of Hg^+ and $[Ru(II)(bpy)_3]^{2+}$, thus acting as a reductive quencher and an electron donor. Afterwards, dimerization of Hg^+ to "Hg_2^{2+}" and subsequent disproportion into Hg(0) and Hg^{2+} may occur, the latter acting as oxidative quencher of the excited state of $[Ru(bpy)_3]^{2+*}$.[82–84] As described by Pfeffer et al., activation of $[(tbbpy)_2Ru(tpphz)PtI_2]^{2+}$ by Hg(0) cannot be excluded, supporting the above mentioned hypothesis that elemental mercury may also act as an electron donor during photocatalysis.[60]

To prevent this side effect, analysing the aliquots of the solution during catalysis without addition of Hg(0) is highly important. Hammarström et al. carried out intensive investigations on the $[(bpy)_2Ru(DMB)PdCl_2]^{2+}$ (DMB = 4′,4‴-((2,5-dimethoxy-1,3-phenylene)bis(ethane-2,1-diyl))bis(4-methyl-2,2′-bipyridine)) system, where the PS and CC are connected via a non-conjugated BL (see Figure 11). They could show that their complex efficiently formed Pd colloids as analysed by transmission electron microscopy (TEM) and X-ray photoelectron spectroscopy (XPS), respectively, switching the system from a molecular to a heterogenous one.[70] Jiang et al. also could show that for their metal–organic framework (MOF) and N,N-chelating ligand based Ir(III)-Pd(II)-system (UiO-67-Ir-PdX_2 with X = acetate or trifluoro-acetic acetate) the CC was reduced during organometallic catalysis (e.g. decarboxylative coupling reaction, no H_2 formation) from Pd(II) to Pd(0). To prevent Pd(0) particle formation, they utilized stoichiometric amounts of Ag_2CO_3 as an oxidant or the irradiation of an Ir-PS/O_2 mixture for reoxidation which significantly enhances overall catalytic activity.[85] It is important to note that the size of the particles is the limiting factor for detection with TEM and for analysing their chemical composition via XPS. To clearly identify if molecular or heterogeneous catalysis takes place, a combination of multiple analysis techniques (e.g., Hg-test, TEM images and DLS experiments) is needed. However, it is also necessary to understand and predict why many intramolecular systems promote particle formation, and only few examples seem to be stable under reductive conditions.[58,60,61,86]

To understand the underlying mechanism for H_2 evolution by di- or oligonuclear systems, i.e., molecular or colloid-driven, analysis of mononuclear noble metal complexes as model systems might yield structure-property-stability relationships, which in turn might open concepts that later can be transferred to di- or oligonuclear complexes.

4.1. Stability of mononuclear catalysts

In many reports, the photocatalysts were typically tested with respect to their stability against visible (or UV) light (as done by photodecomposition studies in pure solvent) to exclude instability during irradiation. Based on these results, it is often concluded that the (photo)catalyst is stable under the applied conditions. However, during catalysis, the presence of an electron donor, ensuring reductive conditions, and an increase in product concentration (e.g. H_2) might influence the stability of the catalyst significantly. To evaluate the influence of these conditions on the systems' stability, it is also important to determine the stability against pure hydrogen, which partially mimics the above-described catalytic scenario, i.e., reductive conditions during photocatalysis in presence of electron donors.

For example, Sakai and co-workers tested the stability of neutral $[Pt(NH_3)_2Cl_2]$ and $[PtCl_2(en)]$ complexes (en = ethane-1,2-diamine) against reduced methylviologen ($MV^{\bullet+}$), as well as

1 atm. of hydrogen (see Figure 4). Interestingly, they could clearly identify that amine stabilized Pt(II)Cl_2 complexes were instable under 1 atm. of H_2 – and efficiently formed Pt particles – but are stable in presence of reduced $MV^{\bullet+}$.[87,88] This indicates that the reducing power of $MV^{\bullet+}$ is insufficient to reduce the Pt(II) centre to Pt(0). According to this assumption, particle formation may only occur at the Pt(0) state and not via a potential Pt(I) intermediate, comparable to the Pd-systems, as Jiang et al. could prevent particle formation by reoxidation of Pd(0) to Pd(II) in Ru-MOF-systems.[85]

However, lowering the amount of H_2 to 500 ppm stabilized the catalytic system and no particle formation was observed for any of the above-mentioned $PtCl_2$ systems, clearly indicating a H_2-concentration dependent instability.[75] As a result, is important to realize that the solubility of H_2 in water (K_H(298 K) = $7.036 \cdot 10^{-3}$ MPa) is significantly higher than its solubility in acetonitrile (K_H(298 K) = $0.545 \cdot 10^{-3}$ MPa). For example, a value of dissolved H_2 in water of 810 µM at 20 °C is found, often one order of magnitude higher than most catalyst concentrations.[89,90] From this perspective, low water contents would be desirable, but systems with high water concentrations may show higher activity due to the presence of more readily available protons.[90]

Based on these results, it is important that the H_2 concentration in solution should be as low as possible to prevent decomposition. Already in 1985 Whitesides et al. demonstrated that [(1,5-COD)Pt(CH_3)$_2$] (1,5-COD = 1,5-cyclooctadiene) can decompose after an induction period which is assigned to Pt(0) formation in presence of H_2. After initial decomposition, Pt(0) is subsequently capable of reducing 1,5-COD to cyclooctane by consumption of H_2. As a consequence, the Pt(0) particles may act as catalysts for the further, autocatalytic deactivation of the catalyst.[74,91,92]

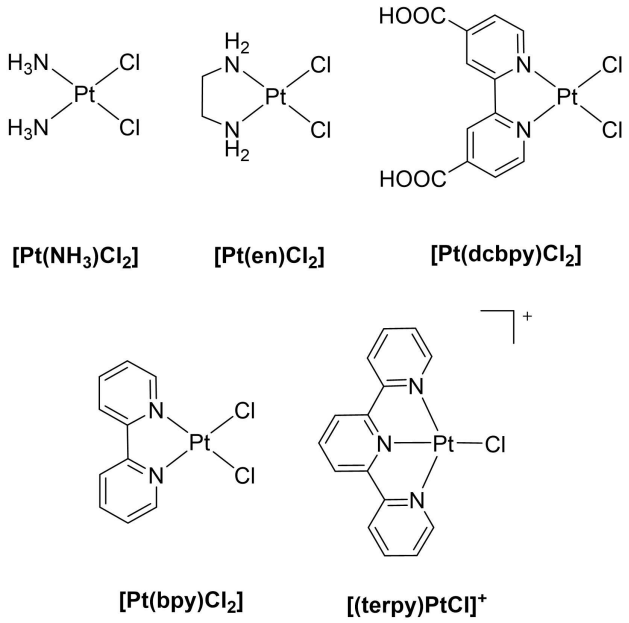

Figure 4. Investigated Pt(II)-complexes on their stability against H_2.

Interestingly, Sakai and co-workers also concluded that the higher flexibility of [Pt(NH_3)$_2$$Cl_2$] and [$PtCl_2$(en)] causes lowering of the barriers for decomposition. According to this, N,N-chelating polypyridyl type complexes (e.g. $[Pt(terpy)Cl]^+$ (terpy = 2,2′:6′,2″-terpyridine) and [Pt(dcbpy)Cl_2] (dcbpy = [2,2′-bipyridine]-4,4′-dicarboxylic acid)) were stable under 1 atm. of H_2 due to a strengthening of the Pt–N bonds by π-back donation.[87]

Eisenberg et al., on the other hand, observed decomposition of [Pt(dcbpy)Cl_2] in the presence of TiO_2 and TEOA (TEOA = triethanol-amine) after irradiation with UV light. Thus, it appears that it is necessary to consider not only the structural aspect of electron-poor ligands that allow back-bonding to stabilize the Pt centers under reductive conditions, but also the involvement of excited states of reduced Pt complexes during irradiation.[79] Moreover, addition of Hg(0) to the one-component system consisting of 0.4 mM $[(terpy)PtCl]^+$ acting at the same time as catalyst and photosensitizer dissolved in a 0.1 M MES buffer (MES = 2-morpholinoethane-1-sulfonic acid) solution (pH 5) and 30 mM EDTA (EDTA = 2,2′,2″,2‴-(ethane-1,2-diyldinitrilo)tetraacetic acid) as sacrificial electron donor resulted in a drop of catalytic activity by only ca. 30%. Okazaki and co-workers concluded that this system containing $[(terpy)PtCl]^+$ as a catalyst and the PS operates in a molecular fashion.[62] Interestingly, by increasing the catalyst concentration, a quadratic dependency on catalytic activity was observed, which may be explained by a dinuclear pathway due to the dimerization of $[(terpy)PtCl]^+$ and formation of $[(terpy)PtCl]_2^{2+}$.[62,95] However, it is also possible that proton reduction occurs on two individual Pt centres by bridged hydrogen atoms (e.g., formation of hydride species).[96]

It should be noted that the observation of an induction period in catalysis often correlates with the initial formation of the active catalyst, which sometimes is the colloidal species. In turn, the lack of an induction period often correlates with a molecular mechanism.[58,70,97]

In the first case, the initially employed systems would only serve as pre-catalysts (e.g., for particle formation).[79,98] In the latter case, these molecular photocatalysts, which efficiently form dimeric species by metal-metal bond formation, can then promote light-driven water reduction.

Until now, it has not been completely understood how the hydrogen formation at the Pt-CC proceeds. One hypothesis is, that a concerted attack of protons and electrons on the platinum catalytic centre occurs which involves the d_{z^2} orbital (already filled in the Pt(II) species) as well as the $d_{x^2-y^2}$ (or better $\sigma_{4(Pt/Pd)}^*$) populated upon (photo)reduction (see Figure 10). Consequently, a Pt(III)-H intermediate, possibly involving a second Pt-centre, forms.[93,94,99,100]

Thus, Ogawa and co-workers performed quantum chemical simulations at the density functional level of theory (DFT) for the catalytic mixture of methylviologene, $[Ru(bpy)_3]^{2+}$, [Pt(5,5′-bcbpy)Cl_2] (5,5′-bcbpy = 5,5′-bis(carbamoyl)-2,2′-bipyridine) and [$PtCl_2$(en)] in aqueous media (see Figure 5). They were able to demonstrate that introduction of electron withdrawing groups stabilize the Pt(III)-H species. Formation of this intermediate is accompanied by elongation of the N,N-chelating metal-ligand

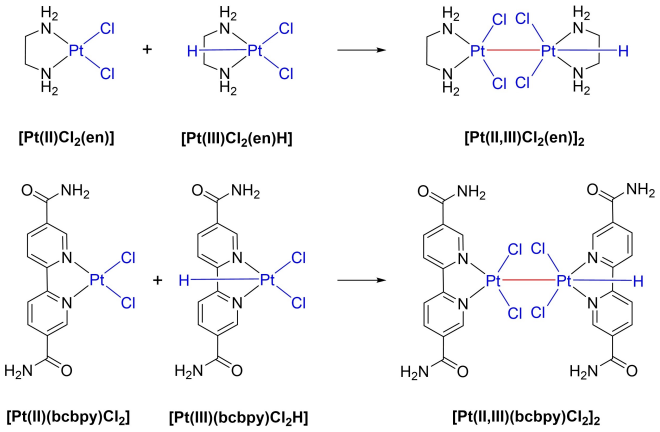

Figure 5. Possible dimerization route of the Pt(II)-precursor and a Pt(III)-hydride according to Sakai et al.[93,94]

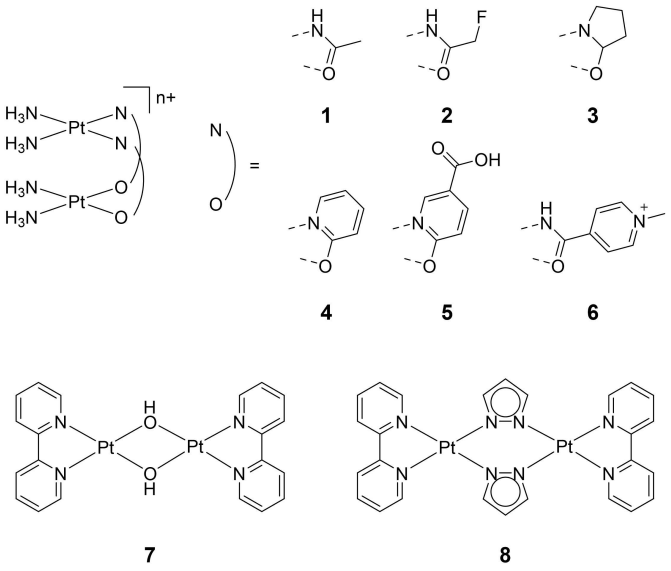

Figure 6. Intradimeric Pt–Pt compounds with varying Pt–Pt-bond distance investigated by Sakai and Ozawa.[99]

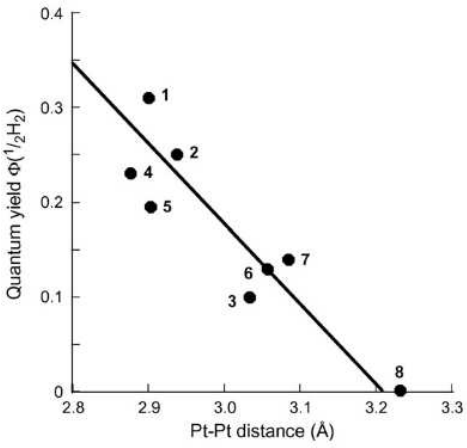

Figure 7. Catalytic activity of intradimeric Pt–Pt compounds investigated by Sakai and Ozawa.[99] Reproduced from Ref. [99] Copyright 2007, with permission from Elsevier.

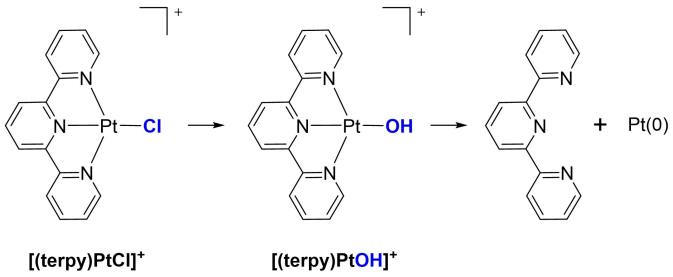

Figure 8. Possible deactivation pathway by terminal ligand exchange at the Pt(II)-centre.

bond (Pt–N_{en} = 2.07 Å and H–Pt–N_{en} = 2.383 Å and 2.119 Å vs. Pt–N_{dcbpy} = 2.034 Å and H–Pt–N_{dcbpy} = 2.269 Å and 2.146 Å) as well as the metal-chloride bond (Pt–Cl_{en} = 2.457 Å and H–Pt–Cl_{en} = 2.473 Å and 2.704 Å vs. Pt–Cl_{dcbpy} = 2.445 Å and H–Pt–Cl_{dcbpy} = 2.524 Å and 2.658 Å) due to transfer of the electron from the PS into the antibonding $\sigma_{x^2-y^2}$* orbital (see $\sigma_{(Pt)}$* exemplarily in Figure 10).[101]

As the Pt–Cl bond in [$PtHCl_2$(en)] is longer than that in [$PtHCl_2$(5,5′-bcbpy)], cleavage of the chloride ligand during photocatalysis is more favourable for [$PtHCl_2$(en)] (see Figure 5). This results in a higher instability of this complex compared to [$PtHCl_2$(5,5′-bcbpy)] as ligand exchanges might initiate reaction sequences leading to colloid formation.[99,100]

However, concomitant formation of Pt–Pt-dimers out of mononuclear complexes by dimerization of a monoreduced and protonated Pt(III)-H species with the non-reduced Pt(II) is in principle possible.[93,94]

Thus, the catalytic activity of multinuclear Pt–Pt catalysts strongly depends on the distance between both platinum centres (see Figures 6 and 7), as a smaller distance enhances catalytic activity by facilitating the formation of these H-bridged intermediates.[101] Furthermore, stronger destabilization of the HOMO in dinuclear Pt_2 compounds enhances catalytic activity.[99] Sakai and Ozawa could clearly demonstrate that in intradimer Pt–Pt catalysts catalytic activity strongly depends on the Pt–Pt-bond length.[99] However, it is tempting to speculate that smaller distances of two Pt-centres raise the possibility for the above-mentioned colloid formation.

Instead of the formation of Pt–Pt bonds, dissociation and subsequent exchange of the terminal halide ligands at the catalyst (e.g. chloride) may also occur. For [(terpy)PtCl]$^+$, Sakai et al. demonstrated that [(terpy)PtCl]$^+$ reacts within the first 30 min to form the respective hydroxo species [(terpy)Pt(OH)]$^+$. 90 min of irradiation resulted in EDTA:Pt mixtures, and at the same time, free terpy ligand starts to appear in ESI-TOF MS, indicating decomposition and particle formation as the final result (see Figure 8).[62]

It is therefore suggested that ligand exchange reactions at the CC initiate the decomposition by opening various reaction pathways.

Based on this knowledge, Sakai and co-workers could show that the addition of salts (e.g., NaCl) to a catalytic solution of $[PtCl_2(dcbpy)]\cdot H_2O$ significantly enhances catalytic activity by switching the equilibrium from the decomposition-tending hydroxo-ligated to the chloride-bound species $[(terpy)PtCl]^+$ which is much more active in hydrogen evolution.[99] This might be due to the fact that the chlorinated species is less prone to decomposition because the time in which the CC stays in its reduced state is significantly shortened.

As mentioned above, the addition of an excess of anions sometimes provides a strong influence on catalytic activity. The electron density of the d_{z^2} orbital at the CC is well-known to strongly correlate with the efficiency of the catalytic system as it stabilizes the formation of Pt(III)-H intermediates.[58,61] For example, typical $Pt(II)Cl_2$ based photocatalysts only provide low catalytic activity in the range of up to 10 TONs.[35,86,102,103] Moreover, exchange of the chloride ligand for neutral ones (e.g., $[Pt(NH_3)_4]^{2+}$, $[Pt(bpy)_2]^{2+}$) leads to a complete loss of catalytic activity, indicating that suitable donor ligands at the CC are necessary.[99]

As a result, $[Pt(SC(NH_2)_2)_4]^{2+}$ showed higher catalytic activity than $[Pt(bpy)_2]^{2+}$, which may be attributed to the strong donor property of the $SC(NH_2)_2$ ligand destabilizing the Pt d_{z^2} orbital which correlates with an enhanced catalytic activity.[99]

Instead of the loss of a halide ligand and subsequent decomposition, one further decomposition route was predicted by Park et al., as they analysed MOFs on their photocatalytic activity. They observed that in the case of Pt(II)-diimine (e.g. $[Pt(bpy)Cl_2]$) bound to a MOF, the Pt centre undergoes decomposition by two-fold reduction of the Pt $\sigma_{4(Pt)}$* (see Section 3 and Figure 10). Thus, such reduction leads to the cleavage of the Pt-diimine bonds and terminates molecular catalysis.[29,79,92] In the square planar confirmation, only electron transfer into $\sigma_{4(Pt)}$* is possible as the d_{z^2} orbital is already filled, causing a switch to a tetrahedral confirmation at which two-fold proton-coupled electron-transfer (PCET) steps might occur, eventually yielding the formation of molecular hydrogen.

To circumvent the detrimental two-fold reduction of the $\sigma_{4(Pt)}$* MO and consequently enhance catalytic activity, the introduction of an electron reservoir in the ligand backbone might represent a viable solution. To integrate a suitable electron reservoir into the ligand structure, it is important to adjust the electronic properties of substituents to enable the lowering of the ligand-based LUMO. Park et al. introduced two tetraphenylsilyl (TPS) substituents to a bpy-based Pt(II) centre (see Figure 9). Compared to the non-TPS containing $[PtCl_2(dmbpy)]$ (dmbpy = 4,4′-dimethyl-2,2′-bipyridine), the electron reservoir significantly enhanced catalytic activity (TON_{TPS} ca. 18,000 compared to TON_{dmbpy} of ca. 60 after 100 h). Ultimately, the TPS moiety allowed an overall TON of 510,000 to be reached within 18 days. Utilization of the Hg test indeed revealed molecular catalysis.[29]

Furthermore, it is important to note that substitution of the direct coordination sphere of the Pt(II)-centre in dinuclear Pt(II) complexes (e.g. Figure 6, structures 1 and 2) with electron withdrawing groups (e.g., fluorine) lowers the HOMO which correlates with the elongation of the Pt–Pt distance and lower catalytic activity.[99]

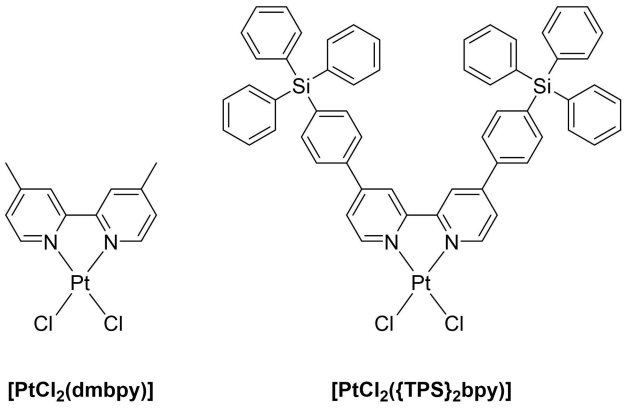

Figure 9. Introduction of the TPS unit significantly enhances catalytic activity compared to structural analogue $[PtCl_2(dmbpy)]$.[29]

As shown in this chapter, multiple deactivation pathways can play a role in Pt- and Pd-catalyzed hydrogen evolution reactions. Therefore, it is very important to sufficiently evaluate the stability of the systems and to analyse the species involved in photocatalysis, as otherwise a rational prevention of decomposition is not possible.

4.2. Stability of di- and oligonuclear catalysts

Transferring the results from mono- to di- and oligonuclear catalysts, it is important to rationalize molecular or colloid-driven hydrogen evolution in di- and oligonuclear photocatalysts as well. The complex $[(tbbpy)_2Ru(tpphz)PdCl_2]^{2+}$ (tbbpy = 4,4′-di-*tert*-butyl-2,2′-bipyridine and tpphz = tetrapyrido[3,2-a:2′,3′-c:3″,2″-h:2‴,3‴-j]phenazine) for example acts as pre-catalyst. Pfeffer et al. could show that $[(tbbpy)_2Ru(tpphz)PdCl_2]^{2+}$ undergoes reduction of the Pd(II)-centre generating a Pd(0) species which is associated with an observed dissociation of a chloride ligand (see Figure 12).[60,67,104] Following the photocatalysis in situ with X-ray absorption near-edge structure measurements (XANES) revealed insights into the catalytic mechanism. This method showed that a large percentage of a metallic (colloidal) Pd-species under photocatalytic conditions was formed. Contrastingly, exchanging the $Pd(II)Cl_2$-centre for a $Pt(II)Cl_2$-centre in the tpphz-bridged system no longer lead to a loss of the CC and formation of colloidal particles. A surprisingly stable coordination of the Pt centre during photocatalysis was observed.[60] A detailed theoretical investigation was conducted to explore the differences in stability and catalytic activity between $[(tbbpy)_2Ru(tpphz)PtCl_2]^{2+}$ and $[(tbbpy)_2Ru(tpphz)PdCl_2]^{2+}$.[68]

Time-dependent DFT (TDDFT) calculations in combination with Marcus theory of electron transfer, were utilised to model the electron transfer from the $^3MLCT_{BL}$ state to the catalytic

centre. This process corresponds to electron transfer from a $\pi_{(BL)}$* orbital on the bridging ligand to the unoccupied $\sigma_{4(Pt/Pd)}$* orbital (Figure 10) on the catalytic centre, forming a charge separated state with a formal Pd(I) and a reduced Pt(II) coordination unit as intermediates. In the investigated Pd(II) and Pt(II) complexes, this $\sigma_{4(Pt/Pd)}$* is the only MO available at the CC that can be populated upon electron transfer as all other orbitals involving the metal centre are already occupied two-fold, see Figure 10. The computational results revealed that although this CS (charge separated) pathway was energetically accessible in the Pd(II)Cl_2 species, the electron transfer rate was slow.[68] In addition, population of Pd-centred ^{3}MC states is highly exergonic and competes with the electron transfer. It is associated with an excitation of an electron from an occupied $d_{(Pd)}$ orbital to the anti-bonding $\sigma_{4(Pt/Pd)}$* orbital (Figure 10), reducing the sigma character of the Pd–Cl bond order and thereby lengthening and weakening it. Following dissociation of a single chloride ligand, the resulting $[(tbbpy)_2Ru(tpphz)PdCl]^{3+}$ species was also investigated and showed significant stabilisation of the CS state, compared to the parent complex. Consequently, chloride ligand dissociation then promotes more efficient CS, which may in turn result in further ligand loss and eventual formation of the metal colloids observed experimentally (see chapter 3 for details). As stated previously, the Pt(II)Cl_2 complex on the other hand, is stable and no ligand dissociation is observed; thus, the addition of access chloride ion source has no effect on catalytic activity. However, the catalytic activity is markedly lower.[60] A further theoretical investigation found that in comparison to Pd(II)Cl_2, the CS states are even higher in energy, making them inaccessible upon visible light excitation, which may correspond to the observed decrease in catalytic activity. Moreover, also the respective ^{3}MC states in the Pt(II)Cl_2 complex reside much higher in energy and are less readily populated reducing the likelihood of ligand dissociation. These computational findings align with the higher stability but lower catalytic activity observed in the Pt(II)Cl_2 species.[57,69] As proposed by Sakai and co-workers a different catalytic mechanism may be operational, i.e. a simultaneous attack by a proton and reduction of the platinum centre, resulting in a penta-coordinated intermediate. This process might potentially involve the assistance of an additional platinum centre. Figure 10 visualizes the reactivity of CC by means of the MOs for a series of potential photoactive supramolecular dyads. As shown, the energy levels of occupied Pd or Pt-centred orbitals show a weak dependency of the halide (X = Cl, Br, or I), while the electron acceptor capacity of is gradually increased from $PtCl_2$ to PtI_2 and even further from $PdCl_2$ to PdI_2 as shown by means of the $\sigma_{4(Pt/Pd)}$* orbital. In consequence, the driving force for the formation of the CS intermediate is enhanced significantly, while as mentioned above, also the tendency for ligand loss and the formation of aggregates is enhanced. Thereby, these quantum chemical simulations suggest that degradation and catalytic activity go hand in hand for palladium-based CC. As no instability of the PtI_2 unit has been observed, and even multiple repair cycles of the corresponding $[(tbbpy)_2Ru(tpphz)Pt(II)I_2]^{2+}$ photocatalyst could be performed without evidence of an altered CS sphere, a different mechanism of catalytic activity seems to operate here.

Subsequent studies for Ru(Cl) catalytic centres for WOC catalysis at a series of bipyridine and oligopyridophenazine ligands, including the tpphz ligand, clearly demonstrated that π-conjugation of the BL can significantly strengthen the metal-

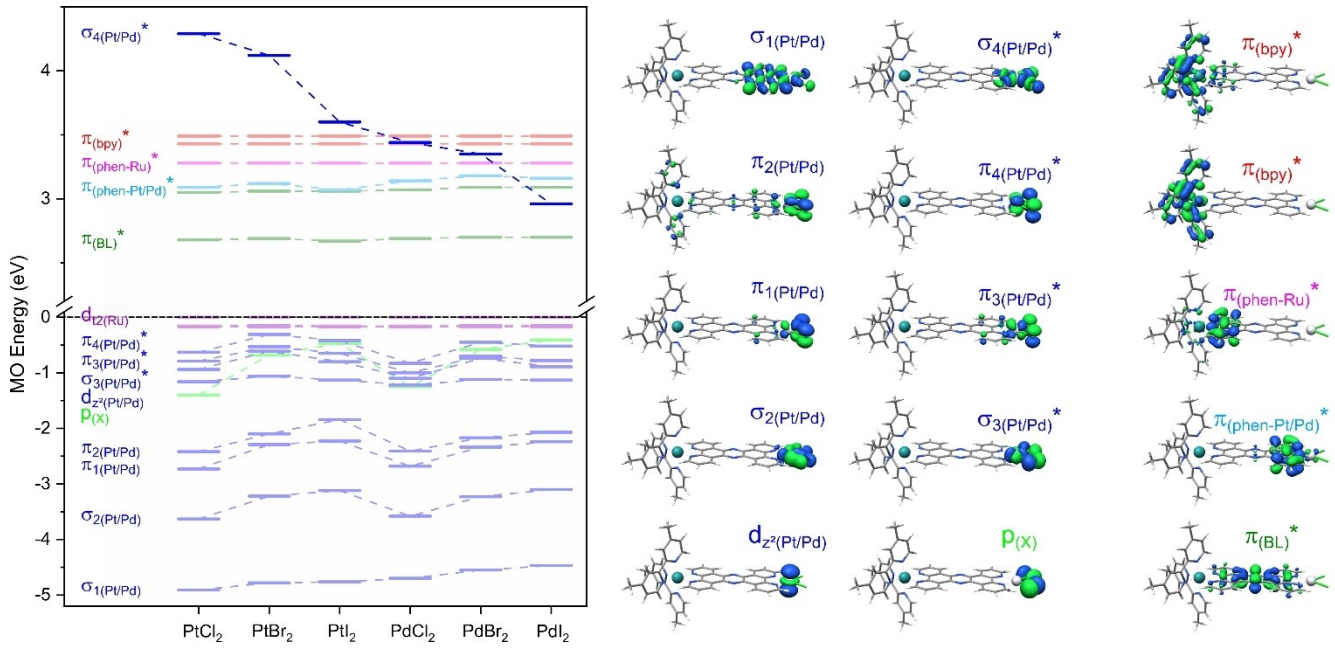

Figure 10. Energy levels of molecular orbitals (Mos) key to the electron transfer of $[(tbbpy)_2Ru(tpphz)MX_2]^{2+}$ (M=Pt or Pd; X=Cl, Br or I). Mos, shown exemplarily for M=Pt and X=Cl, involving the CC are visualized in blue, lone-pairs of the halide are depicted in green; furthermore π* orbitals of the BL (phen: magenta and light blue; phz: olive) as well as of the bipyridine ligands (red) are illustrated The $\sigma_{4(Pt/Pd)}$* orbital, mainly involving M's $d_{x^2-y^2}$ in a classic ligand field theory picture, functions as electron acceptor in the light-induced reduction and is correlated to the stability of the CC (highlighted).

halide bond and subsequently prevent the system to undergo loss of the ligand sphere accompanied by particle formation.[105] However, in the case of $[(tbbpy)_2Ru(tpphz)MCl_2]^{2+}$ (M = Pt or Pd) only the Pt(II)-system seems to provide sufficient stability. Thus, it is tempting to speculate that the different electronic properties of the systems, resulting from the different nature of the CC, have a significant influence on the stability of the photocatalyst during reductive catalysis. As discussed for mononuclear complexes, electron rich ligands without a reservoir cause a labile BL–Pt bond and thus increase the likelihood of forming metal colloids leading to a quasi-heterogeneous mechanism.

A recent report on a related Ru–Pt-based photocatalyst, $[(tbbpy)_2Ru(phenphen)PtCl_2]^{2+}$ (phenphen = 5,5′-bis(1,10-phenanthroline), see Figure 12), an intramolecular photocatalyst without a reservoir and an electron rich ligand moiety at the CC, showed light-driven hydrogen evolution. However, this catalysis is mainly driven by Pt(0) particles, while the tpphz-system which provides an electron deficient BL and thus acts as molecular catalyst in case of $PtCl_2$ as CC.[81]

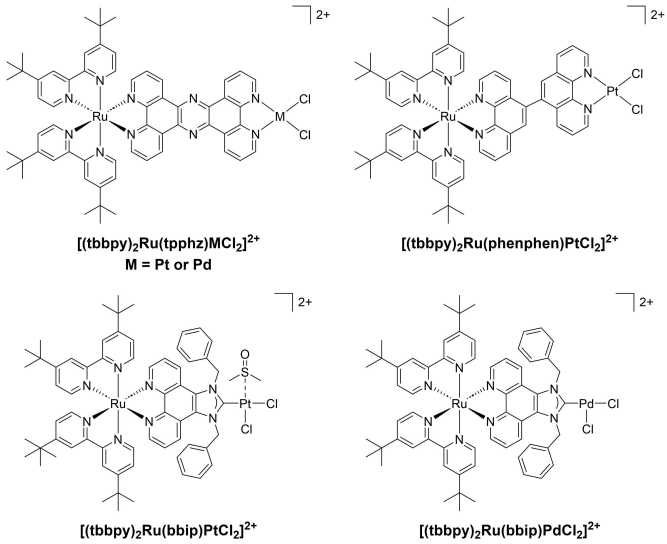

Figure 11. Structures investigated by Brewer et al. and Hammarström et al.[70,106–109]

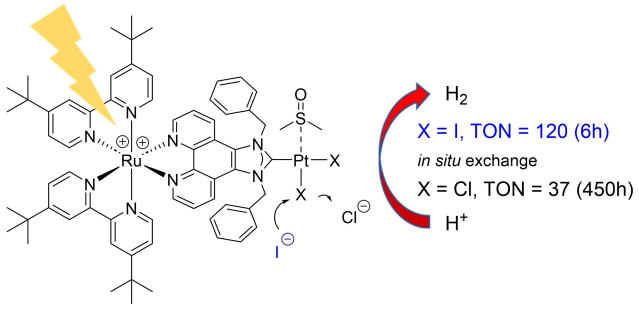

Figure 12. Structures of the investigated RuPt/Pd complexes by Rau et al.[49,59–61,81]

Also, the tetranuclear complexes (Figure 11) investigated by Brewer et al. possessing electron-poor ligand environments at the CC are stable during catalysis and act as molecular photocatalysts, as proven by the Hg test.[106–108] Interestingly, in these systems, three Ru-PS cores significantly lowered catalytic activity compared to the same system based on two Ru-cores, as the TON was decreased by a factor of four.[106]

An alternative approach to stabilizing the CC is changing the CC coordinating donor functionality from pyridine-based N-donors. The synthetic challenge of creating such novel bridging ligands was first mastered by Peuntinger et al. who generated a NHC binding sphere for CCs. Using dynamic light scattering (DLS), they observed high stability during light-driven hydrogen formation by $[(tbbpy)_2Ru(bbip)PdCl_2]^{2+}$ (bbip = 1,3-dibenzyl-1*H*-imidazo[4,5-*f*][1,10]penanthroline-3-ium). Furthermore, no induction period and a relatively stable TOF during the period of active catalysis were observed, additionally indicating a molecular mechanism.[59] This clearly highlights that changing the ligand environment at a given CC (here: Pd) enables its stabilization and molecular hydrogen evolution.

Interestingly, during the irradiation of heterodinuclear RuPt and RuPd complexes under catalytic conditions, the CC may undergo side reactions during light-driven hydrogen evolution. As clearly shown by our group, substitution of the terminal chloride ligand in $[(tbbpy)_2Ru(bbip)PtCl_2]^{2+}$ by methoxy ligands is in principle possible.[58]

According to the ideas of Sakai et al. for stabilizing the CC, the addition of 2000 equiv. of simple salts (e.g., NaCl or TBACl ($N(C_4H_9)_4Cl$)) to the catalytic mixture of $[(tbbpy)_2Ru(tpphz)PtCl_2]^{2+}$ or $[(tbbpy)_2Ru(bbip)PtCl_2]$ might cause an increase in the catalytic activity, as the deactivation route by substitution of one chloride by a hydroxo ligand can be limited (see Figure 7).[60,99]

However, no influence of excess chloride was observed, clearly indicating different mechanisms of the dinuclear complexes and highlighting the fact that in the dinuclear Ru–Pt complexes, potential Cl loss does not seem to interfere with catalytic activity.[60]

In addition, utilization of excess TBACl ($[N(C_4H_9)_4Cl$) for $[(tbbpy)_2Ru(tpphz)PdCl_2]^{2+}$ causes complete deactivation of the catalytic process. In the resting state, a Ru(III)-phenanzine$^{(-\bullet)}$-Pd(II) radical intermediate is formed, and no Cl-ligand dissociation from the Pd-CC and reduction to Pd(I) occurs, which is a required step for hydrogen evolution catalysis for this type of compound as described above.[67]

Changing the chloride ligands in $[(tbbpy)_2Ru(tpphz)PtX_2]^{2+}$ for iodide ligands is not as facile as described for $[(tbbpy)_2Ru(bbip)PtCl_2]$, where simple addition of excess iodide causes chloride-iodide exchange at the CC (see Figure 13).[58,81] For the tpphz system, a different synthesis strategy has to be employed to introduce iodide ligands, as dynamic exchange of the halide ligands in $[(tbbpy)_2Ru(tpphz)PtX_2]^{2+}$ is not possible.

The effect of the halide ligands on light-driven catalysis is very pronounced. Exchange of chlorido- to iodido- ligands leads to an enhancement of the catalytic activity by almost a factor of 40 for the tpphz-based system ($TON_{PtCl2} = 7$ to $TON_{PtI2} = 276$).[61] The addition of TBACl to the very active $[(tbbpy)_2Ru$-

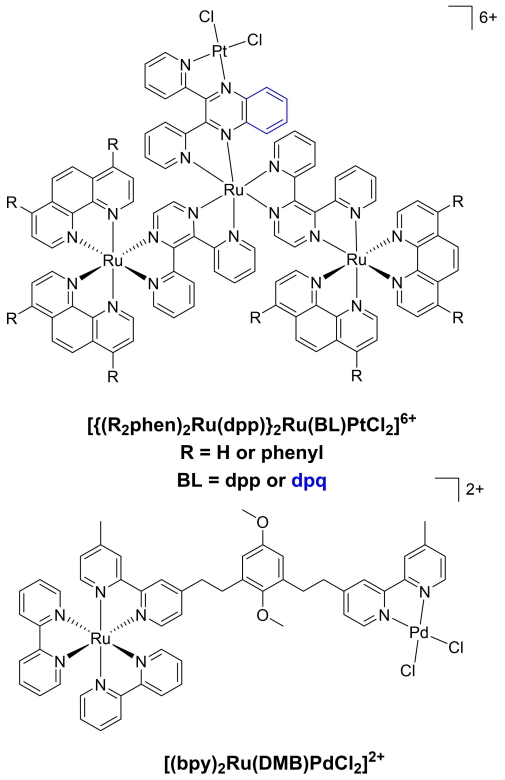

Figure 13. Exchange of the coordinated halide ligand from chloride to iodide via addition of TBAI.[58]

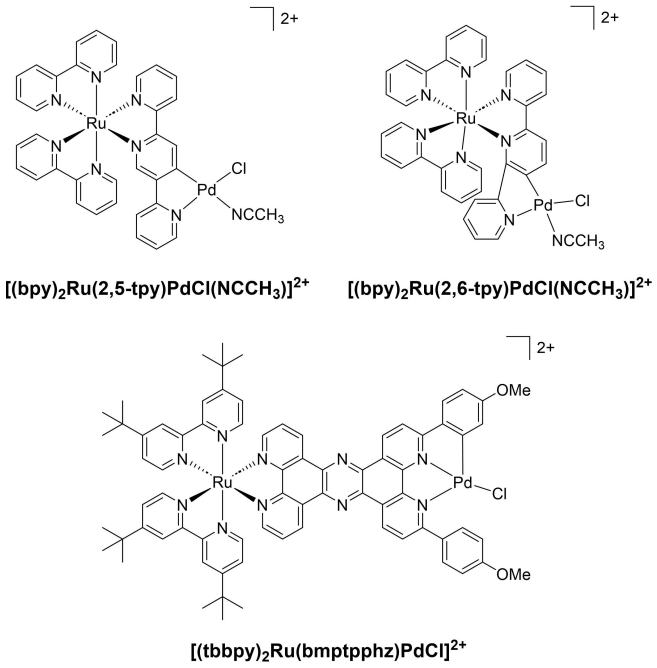

Figure 14. N,C-chelating coordination sites at dinuclear photocatalysts containing Pd-CCs.[110,111]

$(tpphz)PtI_2]^{2+}$ does not lead to any change in catalytic activity, highlighting the very high stability of the Pt–I bond. However, it was also shown that $[(bpy)_2Ru(tpy)PtI_2]^{2+}$ (tpy = 2,2′:5′,2″-terpyridine) can form pentanuclear structures in the solid state by Pt–I–Pt–I–Pt bridges, highlighting that more than one CC species might be present during catalysis.[112] Noteworthily, it was also observed for structural analogue $PdCl_2$ based catalytic systems, that multimetallic catalytic active species might be present in the solid state.[111] Furthermore, the intermolecular approach by mixing $[(bpy)_2Ru(tpy)]^{2+}$ with $[Pt(CH_3CN)_2I_2]$ always resulted in particle formation, while the pentanuclear complex only forms small amounts of metal particles under catalytic conditions.[112]

The higher stability of C,N-chelating BL was also observed by Bindra et al., showing that the stability of the CC strongly depends on the BL architecture, as the RuPd catalyst equipped with the 2,6-tpy BL was stable and inactive while the photocatalyst with a 2,5-tpy BL evolved hydrogen based on a heterogeneous colloidal mechanism (see Figure 14).[111]

Interestingly, Bindra et al. could also show that the peripheral ligands at the Ru-core tremendously influence catalytic activity based on the substitution pattern (e.g., H vs. CO_2Et). For example, the introduction of an carboxylate enhances the catalytic activity by up to one order of magnitude.[112,113] However, until now, it has not been completely clear why this effect is observed.

Based on these results, the future design of stable, molecularly operating oligonuclear photocatalysts has to consider the strong influence of the BL architecture on the stability of the CC. Pt-CCs can be stabilized by equipping ligand spheres with electron reservoir sites or electron withdrawing substituents, while Pd colloid formation might be prevented by changing the ubiquitously utilized α-diimine chelating spheres to suitable N,C-coordination motifs. In addition to the results obtained by Bindra et al., our group could show for $[(tbbpy)_2Ru(bmptpphz)PdCl]^{2+}$ (bmptpphz = 3,6-bis(4-methoxyphenyl)tetrapyrido[3,2-a:2′,3′-c:3″,2″-h:2‴,3‴-j]phenazine) that the addition of Hg prior to catalysis causes no depletion of the CC, already indicating a higher stability of the CC by the new coordination environment.[110] However, addition of Hg during catalysis causes complete loss of the catalytic activity. Although the change from N,N-chelating ligands to N,C chelates improve the CC's stability,[111,112] this is even not sufficient to allow molecular light-driven hydrogen evolution in all cases.

As the main influence on electron transfer from the PS to the CC is promoted by the BL architecture as well, it is important to consider balancing the electronic situation at the BL to optimize it on the one hand for forward electron transfer and on the other hand for the stability of the CC, respectively.

For example, the introduction of a phenazine unit as in $[(tbbpy)_2Ru(tpphz)PtI_2]^{2+}$ can indeed cause activation of the catalytic system. It serves as an electronic reservoir prohibiting the two-fold reduction of Pt-based CC and, at the same time as a stabilizing moiety for the ligand sphere at the Pt-centre as described above. However, over the course of several days, it is observed that the phenazine spheres undergo a two-fold reduction during catalysis by the formal addition of one

molecule of H_2, likely via a disproportionation mechanism, stopping the overall catalytic activity.[49] Thus, it is important to find molecular solutions to stabilize the CC and to prevent decomposition and deactivation at the same time.

5. How to Prevent Decomposition/Deactivation and Possible Repair Strategies when the System Stopped Evolving H_2

As shown in chapter 3, it is hard to avoid side reactions during light-driven hydrogen evolution catalysis with Pt- and Pd-based systems involving ligand substitution, reductive processes of the BL and depletion of the CC. To sum up, in principle, every single component consisting of the PS, BL, and CC can undergo decomposition.[99] However, there are different strategies known in literature to prevent decomposition or at least to repair the catalytic system and prolong molecular catalysis.

On the one hand, deactivation often occurs by reversible ligand substitution at the CC (e.g., chloride substitution by hydroxide or neutral ligands). In this case, the addition of halide salts (e.g. NaCl) should switch the equilibrium to the active catalyst and prevent further deactivation (see Figures 8 and 15).[99] On the other hand, light-induced particle formation is an often-observed issue in literature. Therefore, Eisenberg et al. and Park et al. could show that the addition of an excess of free ligand to a nanoparticle forming catalyst can avoid particle formation and significantly enhance molecular catalysis.[92,114,115]

Also in this case, the general principle is based on shifting the equilibrium from the decomposed product to the active catalyst. By varying the excess of ligand, switching the heterogeneous catalysis to homogenous catalysis seems possible.[92] However, for the utilization of PS-BL-CC based architectures such an approach would require a significant excess of PS-BL to accomplish a similar result. This would most likely be a very inefficient approach. It is important to realize that if the catalysis stops after several hours (or days), particle formation is not always involved in the present deactivation pathway.

Thus, not only does decomposition of the catalytically active metal centre occur, but also the BL as well as the PS may degrade over time.[99] As described by our group, also a two-fold reduction of the BL itself can occur, resulting in an ultrafast population of unreactive excited states exclusively localized on

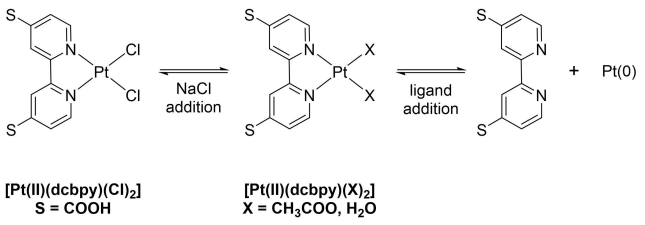

Figure 15. Possible stabilization techniques to prevent ligand loss and subsequent particle formation.

the BL upon photoexcitation.[49,63] It was demonstrated that $[(tbbpy)_2Ru(tpphz)PtI_2]^{2+}$ undergoes reduction of the phenazine sphere forming two secondary amines (see Figure 16).[49] However, reoxidation by in situ formed singlet oxygen can regenerate the aromatic BL and thus the catalysis can be reinitiated.

In this context, it should be noted that only due to the high stability of the Pt centre in this system, resulting from the electron reservoir function of the tpphz BL, is repair of a molecular photocatalyst possible at all. Such an active repair mechanism seems to open a new avenue for the design of functional photocatalysts with extended lifetimes.

6. Final Remarks

Light-driven hydrogen evolution using intramolecular catalysts is of great interest for the direct conversion of visible light into chemical energy. However, transferring the idea of utilizing intramolecular systems consisting of a PS, BL and CC into practice is difficult to realize. To be active in (hydrogen evolution) catalysis, a delicate balance between stability and reactivity is needed, which currently still often leads to irreversible side reactions and concomitant deactivation processes over time.

To successfully prevent particle formation in noble metal-containing catalysts, adjustment of the ligand plays a crucial role. Introduction of electron withdrawing groups can stabilize hydride-based intermediates and prevent halide dissociation at the CC, which might be the first step towards decomposition. Also, exchanging the typically utilized N,N-chelates to NHC ligands or N,C chelating ligands may help to stabilize the CCs. If dissociation still occurs, addition of halide salts may switch the ligand exchange equilibrium beneficially to limit decomposition. In addition to particle formation, also a binuclear (or even

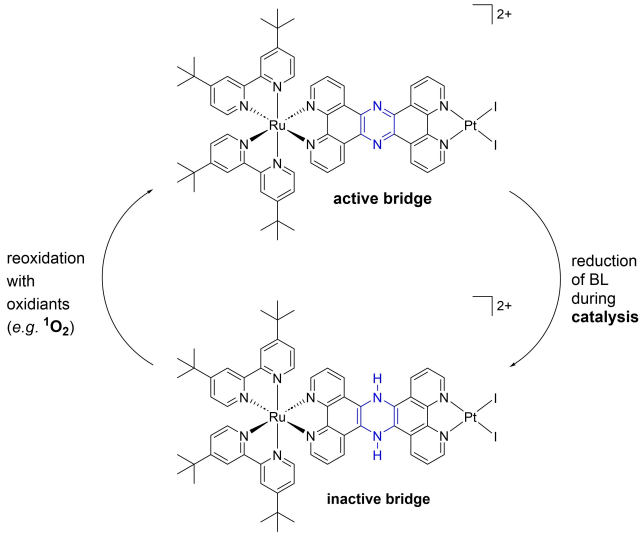

Figure 16. Deactivation of $[(tbbpy)_2Ru(tpphz)PtI_2]^{2+}$ during catalysis by hydrogenation of the phenazine sphere (blue) and possible regeneration of the active catalytic system by reoxidation by strong oxidants (e.g. $^1O_2$).

multinuclear) deactivation mechanism may occur. In this case, catalytic activity might be mainly determined by the Pt–Pt-bond lengths and may be varied by introduction of varying steric substituents. However, short Pt–Pt-distances may also open the possibility for the above-mentioned particle formation. Further it was shown that dissociative ^{3}MC states at the CC are higher for the 5d metal Pt in energy compared to the 4d metal Pd causing higher instability for the respective Pd complexes which are often prone to particle formation while Pt-complexes are typically more stable. It might be that decomposition is indicated by metal(0) species which were not accessible for Pt centres during catalysis, contrary to similar Pd systems. The facile Pd(0) formation may be assisted by the facile reduction-induced loss of the monodentate ligands at the CC which is not observed in analogous Pt-based systems. However, if not equipped with electronically suitable coordination environments, Pt-complexes are often just simple precursors for the active catalyst, typically indicated by an induction period at the beginning of the photocatalytic process.

Therefore, intensive investigations have to be performed to obtain clear structure-property-stability relationships, as only limited conclusions have been drawn so far. This is also due to the fact that not in every system the role of colloids is clarified so far. It is thus suggested that for the various systems that have already been reported and will be reported in future, a variety of tests (Hg-test, microscopy, dynamic light scattering) under standardized conditions should be routinely applied to verify the molecular nature of catalysis.[116,117]

Acknowledgements

M. Lämmle acknowledges support by the Studienstiftung des deutschen Volkes for a PhD scholarship. Furthermore, funding by the Deutsche Forschungsgemeinschaft (German Research Foundation) via the TRR CATALIGHT, Projektnummer 364549901 (A1 and A4), TRR234 and Projektnummer 448713509 is gratefully acknowledged. Open Access funding enabled and organized by Projekt DEAL.

Conflict of Interest

The authors declare no conflict of interest.

Data Availability Statement

Data sharing is not applicable to this article as no new data were created or analyzed in this study.

Keywords: hydrogen · instability · light · photocatalysis · ruthenium

[1] D. A. Lashof, D. R. Ahuja, *Nature* **1990**, *344*, 529–531.
[2] S. A. Montzka, E. J. Dlugokencky, J. H. Butler, *Nature* **2011**, *476*, 43–50.
[3] J. T. Houghton, Y. Ding, D. J. Griggs, M. Noguer, P. J. Van der Linden, X. Dai, K. Maskell, C. A. Johnson, *Cambridnge Univ. Press* **2001**, 10.1126/science.187.4177.646.
[4] J. P. Smol, *Nature* **2012**, *483*, S12.
[5] M. K. Hubbert, *Science* **1949**, *109*, 103–109.
[6] S. H. Mohr, J. Wang, G. Ellem, J. Ward, D. Giurco, *Fuel* **2015**, *141*, 120–135.
[7] H. Ritchie, M. Roser, P. Rosado, "CO_2 and Greenhouse Gas Emissions", can be found under https://ourworldindata.org/co2-and-other-greenhouse-gas-emissions, **2020**.
[8] G. Ciamician, *Science* **1912**, *36*, 385–395.
[9] E. Kabir, P. Kumar, S. Kumar, A. A. Adelodun, K. H. Kim, *Renewable Sustainable Energy Rev.* **2018**, *82*, 894–900.
[10] A. Evans, V. Strezov, T. J. Evans, *Renewable Sustainable Energy Rev.* **2012**, *16*, 4141–4147.
[11] S. Ould Amrouche, D. Rekioua, T. Rekioua, S. Bacha, *Int. J. Hydrogen Energy* **2016**, *41*, 20914–20927.
[12] J. P. Barton, D. G. Infield, *IEEE Trans. ENERGY Convers.* **2004**, *19*, 441–448.
[13] S. Berardi, S. Drouet, L. Francàs, C. Gimbert-Suriñach, M. Guttentag, C. Richmond, T. Stoll, A. Llobet, *Chem. Soc. Rev.* **2014**, *43*, 7501–7519.
[14] J. Barber, P. D. Tran, *J. R. Soc. Interface* **2013**, *10*, 1–15.
[15] K. Mazloomi, C. Gomes, *Renewable Sustainable Energy Rev.* **2012**, *16*, 3024–3033.
[16] G. Nicoletti, N. Arcuri, G. Nicoletti, R. Bruno, *Energy Convers. Manage.* **2015**, *89*, 205–213.
[17] P. E. Dodds, I. Staffell, A. D. Hawkes, F. Li, P. Grünewald, W. McDowall, P. Ekins, *Int. J. Hydrogen Energy* **2015**, *40*, 2065–2083.
[18] I. Staffell, D. Scamman, A. Velazquez Abad, P. Balcombe, P. E. Dodds, P. Ekins, N. Shah, K. R. Ward, *Energy Environ. Sci.* **2019**, *12*, 463–491.
[19] E. Zoulias, E. Varkaraki, *Tcjst* **2004**, *4*, 41–71.
[20] Z. Han, R. Eisenberg, *Acc. Chem. Res.* **2014**, *47*, 2537–2544.
[21] N. Armaroli, V. Balzani, *ChemSusChem* n.d.
[22] S. E. Hosseini, M. A. Wahid, *Renewable Sustainable Energy Rev.* **2016**, *57*, 850–866.
[23] F. Heydemann, *Kritisch für den Naturschutz? Freiflächenphotovoltaik: Grundlagen und Anforderungen*, NABU Schleswig-Holstein **2020**.
[24] D. R. Weinberg, C. J. Gagliardi, J. F. Hull, C. F. Murphy, C. A. Kent, B. C. Westlake, A. Paul, D. H. Ess, D. Granville, T. J. Meyer, *Chem. Rev.* **2012**, 4016–4093.
[25] T. J. Meyer, *Acc. Chem. Res.* **1989**, *22*, 163–170.
[26] D. L. Ashford, M. K. Gish, A. K. Vannucci, M. K. Brennaman, J. L. Templeton, J. M. Papanikolas, T. J. Meyer, *Chem. Rev.* **2015**, *115*, 13006–13049.
[27] B. Probst, C. Kolano, P. Hamm, R. Alberto, *Inorg. Chem.* **2009**, *48*, 1836–1843.
[28] S. Losse, J. G. Vos, S. Rau, *Coord. Chem. Rev.* **2010**, *254*, 2492–2504.
[29] D. R. Whang, S. Y. Park, *ChemSusChem* **2015**, *8*, 3204–3207.
[30] W. R. Mcnamara, Z. Han, P. J. Alperin, W. W. Brennessel, P. L. Holland, R. Eisenberg, *J. Am. Chem. Soc.* **2011**, *133*, 15368–15371.
[31] W. M. Singh, T. Baine, S. Kudo, S. Tian, X. A. N. Ma, H. Zhou, N. J. Deyonker, T. C. Pham, J. C. Bollinger, D. L. Baker, B. Yan, C. E. Webster, X. Zhao, *Angew. Chem. Int. Ed.* **2012**, *51*, 5941–5944; *Angew. Chem.* **2012**, *124*, 6043–6046.
[32] Z. Han, W. R. McNamara, M.-S. Eum, P. L. Holland, R. Eisenberg, *Angew. Chem.* **2012**, *124*, 1699–1702; *Angew. Chem. Int. Ed.* **2012**, *51*, 1667–1670.
[33] Y. Halpin, M. T. Pryce, S. Rau, D. Dini, J. G. Vos, *Dalton Trans.* **2013**, *42*, 16243–16254.
[34] M. Schulz, M. Karnahl, M. Schwalbe, J. G. Vos, *Coord. Chem. Rev.* **2012**, *256*, 1682–1705.
[35] H. Ozawa, M. A. Haga, K. Sakai, *J. Am. Chem. Soc.* **2006**, *128*, 4926–4927.
[36] H. Ozawa, M. Kobayashi, B. Balan, S. Masaoka, K. Sakai, *Chem. Asian J.* **2010**, *5*, 1860–1869.
[37] H. Ozawa, Y. Yokoyama, M. Haga, K. Sakai, *Dalton Trans.* **2007**, 1197–1206.
[38] V. W. Yam, V. W. Lee, K. Cheung, *Organometallics* **1997**, *16*, 2833–2841.
[39] P. Contreras Carballada, N. Mourtzis, M. Felici, S. Bonnet, R. J. M. Nolte, R. M. Williams, L. De Cola, M. C. Feiters, *Eur. J. Org. Chem.* **2012**, 6729–6736.
[40] P. Du, J. Schneider, P. Jarosz, J. Zhang, W. W. Brennessel, R. Eisenberg, *J. Phys. Chem. B* **2007**, *111*, 6887–6894.
[41] P. Du, J. Schneider, P. Jarosz, R. Eisenberg, *J. Am. Chem. Soc.* **2006**, *128*, 7726–7727.
[42] D. K. Dogutan, D. G. Nocera, *Acc. Chem. Res.* **2019**, 3143–3148.

[43] D. Gust, T. A. Moore, A. L. Moore, *Acc. Chem. Res.* **2009**, *42*, 1890–1898.
[44] W. Lubitz, B. Tumas, *Chem. Rev.* **2007**, *107*, 3900–3903.
[45] L. L. Tinker, N. D. McDaniel, P. N. Curtin, C. K. Smith, M. J. Ireland, S. Bernhard, *Chem. Eur. J.* **2007**, *13*, 8726–8732.
[46] C. Förster, K. Heinze, *Chem. Soc. Rev.* **2020**, *49*, 1057–1070.
[47] O. S. Wenger, *J. Am. Chem. Soc.* **2018**, *140*, 13522–13533.
[48] Y. Abderrazak, A. Bhattacharyya, O. Reiser, *Angew. Chem. Int. Ed.* **2021**, *60*, 21100–21115; *Angew. Chem.* **2021**, *133*, 21268–21284.
[49] M. G. Pfeffer, C. Müller, E. T. E. Kastl, A. K. Mengele, B. Bagemihl, S. S. Fauth, J. Habermehl, L. Petermann, M. Wächtler, M. Schulz, D. Chartrand, F. Laverdiére, P. Seeber, S. Kupfer, S. Gräfe, G. S. Hanan, J. G. Vos, B. Dietzek-Ivanšić, S. Rau, *Nat. Chem.* **2022**, *14*, 500–506.
[50] J. Schwarz, A. Ilic, S. Kaufhold, J. Ahokas, P. Myllyperkiö, M. Pettersson, K. Wärnmark, *Sustain. Energy Fuels* **2022**, *6*, 4388–4392.
[51] J. R. Bolton, *Science* **1978**, *202*, 705–711.
[52] R. Matheu, P. Garrido-Barros, M. Gil-Sepulcre, M. Z. Ertem, X. Sala, C. Gimbert-Suriñach, A. Llobet, *Nat. Chem. Rev.* **2019**, 331–341.
[53] B. Limburg, E. Bouwman, S. Bonnet, *Coord. Chem. Rev.* **2012**, *256*, 1451–1467.
[54] N. Kaveevivitchai, R. Chitta, R. Zong, M. El Ojaimi, R. P. Thummel, *J. Am. Chem. Soc.* **2012**, *134*, 10721–10724.
[55] F. L. Huber, S. Amthor, B. Schwarz, B. Mizaikoff, C. Streb, S. Rau, *Sustain. Energy Fuels* **2018**, *2*, 1974–1978.
[56] S. Amthor, S. Knoll, M. Heiland, L. Zedler, C. Li, D. Nauroozi, W. Tobaschus, A. K. Mengele, M. Anjass, U. S. Schubert, B. Dietzek-Ivanšić, S. Rau, C. Streb, *Nat. Chem.* **2022**, *14*, 321–327.
[57] H. Ozawa, K. Sakai, *Chem. Commun.* **2011**, *47*, 2227–2242.
[58] S. Kaufhold, D. Imanbaew, C. Riehn, S. Rau, *Sustain. Energy Fuels* **2017**, *1*, 2066–2070.
[59] K. Peuntinger, T. D. Pilz, R. Staehle, M. Schaub, S. Kaufhold, L. Petermann, M. Wunderlin, H. Görls, F. W. Heinemann, J. Li, T. Drewello, J. G. Vos, D. M. Guldi, S. Rau, *Dalton Trans.* **2014**, *43*, 13683–13695.
[60] M. G. Pfeffer, B. Schäfer, G. Smolentsev, J. Uhlig, E. Nazarenko, J. Guthmuller, C. Kuhnt, M. Wächtler, B. Dietzek, V. Sundström, S. Rau, *Angew. Chem. Int. Ed.* **2015**, *54*, 5044–5048; *Angew. Chem.* **2015**, *127*, 5132–5136.
[61] M. G. Pfeffer, T. Kowacs, M. Wächtler, J. Guthmuller, B. Dietzek, J. G. Vos, S. Rau, *Angew. Chem. Int. Ed.* **2015**, *54*, 6627–6631; *Angew. Chem.* **2015**, *127*, 6727–6731.
[62] R. Okazaki, S. Masaoka, K. Sakai, *Dalton Trans.* **2009**, 6127–6133.
[63] L. Zedler, P. Wintergerst, A. K. Mengele, C. Müller, C. Li, B. Dietzek-Ivanšić, S. Rau, *Nat. Commun.* **2022**, *13*, 2538.
[64] L. Zedler, C. Müller, P. Wintergerst, A. K. Mengele, S. Rau, B. Dietzek-Ivanšić, *Chem. Eur. J.* **2022**, *28*, e202200490.
[65] M. Karnahl, C. Kuhnt, F. Ma, A. Yartsev, M. Schmitt, B. Dietzek, S. Rau, J. Popp, *ChemPhysChem* **2011**, *12*, 2101–2109.
[66] K. Ritter, C. Pehlken, D. Sorsche, S. Rau, *Dalton Trans.* **2015**, *44*, 8889–8905.
[67] S. Rau, B. Schäfer, D. Gleich, E. Anders, M. Rudolph, M. Friedrich, H. Görls, W. Henry, J. G. Vos, *Angew. Chem. Int. Ed.* **2006**, *45*, 6215–6218; *Angew. Chem.* **2006**, *118*, 6361–6364.
[68] M. Staniszewska, S. Kupfer, J. Guthmuller, *Chem. Eur. J.* **2018**, *24*, 11166–11176.
[69] M. Staniszewska, S. Kupfer, J. Guthmuller, *J. Phys. Chem. C* **2019**, *123*, 16003–16013.
[70] P. Lei, M. Hedlund, R. Lomoth, H. Rensmo, O. Johansson, L. Hammarström, *J. Am. Chem. Soc.* **2008**, *130*, 26–27.
[71] N. Toshima, M. Muriyama, Y. Yamada, H. Hirai, *Chem. Lett.* **1981**, 793–796.
[72] P. Keller, A. Moradpour, *J. Am. Chem. Soc.* **1980**, *102*, 7193–7196.
[73] J. Stein, L. N. Lewis, Y. Gao, R. A. Scott, *J. Am. Chem. Soc.* **1999**, *121*, 3693–3703.
[74] G. M. Whitesides, M. Hackett, R. L. Brainard, J. P. M. Lavalleye, A. F. Sowinskl, A. N. Izumi, S. S. Moore, D. W. Brown, E. M. Staudt, *Organometallics* **1985**, *4*, 1819–1830.
[75] V. Artero, M. Fontecave, *Chem. Soc. Rev.* **2013**, *42*, 2338–2356.
[76] D. R. Anton, R. H. Crabtree, *Organometallics* **1983**, *2*, 855–859.
[77] V. M. Chernyshev, A. V. Astakhov, I. E. Chikunov, R. V. Tyurin, D. B. Eremin, G. S. Ranny, V. N. Khrustalev, V. P. Ananikov, *ACS Catal.* **2019**, *9*, 2984–2995.
[78] R. Baba, S. Nakabayashi, A. Fujishimam, *J. Phys. Chem.* **1985**, *89*, 1902–1905.
[79] P. Du, J. Schneider, F. Li, W. Zhao, U. Patel, F. N. Castellano, R. Eisenberg, *J. Am. Chem. Soc.* **2008**, *130*, 5056–5058.
[80] X. Wang, S. Goeb, Z. Ji, N. A. Pogulaichenko, F. N. Castellano, *Inorg. Chem.* **2011**, *50*, 705–707.
[81] M. Lämmle, T. D. Pilz, R. J. Kutta, M. Müßler, A. K. Mengele, H. Görls, F. W. Heinemann, S. Rau, *Dalton Trans.* **2022**, *51*, 15282.
[82] R. L. Wolfgang, R. W. Dodson, *J. Phys. Chem.* **1952**, *56*, 872–876.
[83] I. Sanemasa, *Inorg. Chem.* **1977**, *16*, 2786–2788.
[84] K. Kalyanasundaram, *Coord. Chem. Rev.* **1982**, *46*, 159–244.
[85] J. Li, L. He, Q. Liu, Y. Ren, H. Jiang, *Nat. Commun.* **2022**, *13*, 1–13.
[86] K. Yatsuzuka, K. Yamauchi, K. Sakai, *Chem. Commun.* **2021**, *57*, 5183–5186.
[87] K. Yamauchi, S. Masaoka, K. Sakai, *Dalton Trans.* **2011**, *40*, 12447–12449.
[88] K. Yamauchi, S. Masaoka, K. Sakai, *J. Am. Chem. Soc.* **2009**, *131*, 8404–8406.
[89] R. W. Cargill, A. L. Cramer, M. E. Derrick, J. C. Gjaldbaek, S. A. Johnson, P. L. Long, E. S. Thomsen, D. G. T. Thornhill, E. Wilhelm, *Solubility Data Series, Hydrogen and Deuterium Volume 5/6*, C.L. Young. International Union of Pure and Applied Chemistry, Pergamon Press, **1981**.
[90] Purwanto, R. M. Deshpande, R. V. Chaudhari, H. Delmas, *J. Chem. Eng. Data* **1996**, *41*, 1414–1417.
[91] C. Besson, E. E. Finney, R. G. Finke, *J. Am. Chem. Soc.* **2005**, *127*, 8179–8184.
[92] D. Kim, D. R. Whang, S. Y. Park, *J. Am. Chem. Soc.* **2016**, *138*, 8698–8701.
[93] T. V. O'halloran, P. K. Mascharak, I. D. Williams, M. M. Roberts, S. J. Lippard, *Inorg. Chem.* **1987**, *26*, 1261–1270.
[94] K. Matsumoto, K. Sakai, *Adv. Inorg. Chem.* **1999**, *49*, 375–427.
[95] T. Gill, A. Sadownick, *J. Am. Chem. Soc.* **1975**, *4*, 6159–6168.
[96] J. A. Bailey, M. G. Hill, R. E. Marsh, V. M. Miskowski, W. P. Schaefer, H. B. Gray, *Inorg. Chem.* **1995**, *34*, 4591–4599.
[97] L. N. Lewis, N. Lewis, *J. Am. Chem. Soc.* **1986**, *108*, 7228–7231.
[98] W. T. Eckenhoff, R. Eisenberg, *Dalton Trans.* **2012**, *41*, 13004–13021.
[99] K. Sakai, H. Ozawa, *Coord. Chem. Rev.* **2007**, *251*, 2753–2766.
[100] M. Kobayashi, S. Masaoka, K. Sakai, *Photochem. Photobiol. Sci.* **2009**, *8*, 196–203.
[101] M. Ogawa, G. Ajayakumar, S. Masaoka, H. B. Kraatz, K. Sakai, *Chem. Eur. J.* **2011**, *17*, 1148–1162.
[102] G. Ajayakumar, M. Kobayashi, S. Masaoka, K. Sakai, *Dalton Trans.* **2011**, *40*, 3955.
[103] K. Yamamoto, K. Kitamoto, K. Yamauchi, K. Sakai, *Chem. Commun.* **2015**, *51*, 14516–14519.
[104] T. Kowacs, Q. Pan, P. Lang, L. O'Reilly, S. Rau, W. R. Browne, M. T. Pryce, A. Huijser, J. G. Vos, *Faraday Discuss.* **2015**, *185*, 143–170.
[105] S. Amthor, D. Hernández-Castillo, B. Maryasin, P. Seeber, A. K. Mengele, S. Gräfe, L. González, S. Rau, *Chem. A Eur. J.* **2021**, *27*, 16871–16878.
[106] J. K. White, K. J. Brewer, *Chem. Commun.* **2015**, *51*, 16123–16126.
[107] J. D. Knoll, S. M. Arachchige, G. Wang, K. Rangan, R. Miao, S. L. H. Higgins, B. Okyere, M. Zhao, P. Croasdale, K. Magruder, B. Sinclair, C. Wall, K. J. Brewer, *Inorg. Chem.* **2011**, *50*, 8850–8860.
[108] J. D. Knoll, S. M. Arachchige, K. J. Brewer, *ChemSusChem* **2011**, *4*, 252–261.
[109] G. F. Manbeck, K. J. Brewer, *Coord. Chem. Rev.* **2013**, *257*, 1660–1675.
[110] M. G. Pfeffer, L. Zedler, S. Kupfer, M. Paul, M. Schwalbe, K. Peuntinger, D. M. Guldi, J. Guthmuller, J. Popp, S. Gräfe, B. Dietzek, S. Rau, *Dalton Trans.* **2014**, *43*, 11676–11686.
[111] G. Singh Bindra, M. Schulz, A. Paul, R. Groarke, S. Soman, J. L. Inglis, W. R. Browne, M. G. Pfeffer, S. Rau, B. J. MacLean, M. T. Pryce, J. G. Vos, *Dalton Trans.* **2012**, *41*, 13050–13059.
[112] T. Kowacs, L. O'Reilly, Q. Pan, A. Huijser, P. Lang, S. Rau, W. R. Browne, M. T. Pryce, J. G. Vos, *Inorg. Chem.* **2016**, *55*, 2685–2690.
[113] G. Singh Bindra, M. Schulz, A. Paul, S. Soman, R. Groarke, J. Inglis, M. T. Pryce, W. R. Browne, S. Rau, B. J. MacLean, J. G. Vos, *Dalton Trans.* **2011**, *40*, 10812–10814.
[114] T. Lazarides, T. McCormick, P. Du, G. Luo, B. Lindley, R. Eisenberg, *J. Am. Chem. Soc.* **2009**, *131*, 9192–9194.
[115] T. M. McCormick, Z. Han, D. J. Weinberg, W. W. Brennessel, P. L. Holland, R. Eisenberg, *Inorg. Chem.* **2011**, *50*, 10660–10666.
[116] H. Ozawa, K. Sakai, *Chem. Lett.* **2007**, *36*, 920–921.
[117] M. Kobayashi, S. Masaoka, K. Sakai, *Molecules* **2010**, *15*, 4908–4923.

Manuscript received: August 31, 2022
Accepted manuscript online: February 20, 2023
Version of record online: May 12, 2023